

Pirovano, Giacomo, Ashton, Thomas, Herbert, Katharine ORCID logoORCID: <https://orcid.org/0000-0001-9437-0253>, Bryant, Richard J, Verrill, Clare L, Cerundolo, Lucia, Buffa, Francesca M, Prevo, Remko, Harrap, Iona, Ryan, Anderson J, Macaulay, Valentine, McKenna, William G and Higgins, Geoff S (2017) TOPK modulates tumour-specific radiosensitivity and correlates with recurrence after prostate radiotherapy. British Journal of Cancer, 117. pp. 503-512.

Downloaded from: <https://ray.yorks.ac.uk/id/eprint/9399/>

The version presented here may differ from the published version or version of record. If you intend to cite from the work you are advised to consult the publisher's version: <https://www.nature.com/articles/bjc2017197>

Research at York St John (RaY) is an institutional repository. It supports the principles of open access by making the research outputs of the University available in digital form. Copyright of the items stored in RaY reside with the authors and/or other copyright owners. Users may access full text items free of charge, and may download a copy for private study or non-commercial research. For further reuse terms, see licence terms governing individual outputs. [Institutional Repository Policy Statement](#)

RaY

Research at the University of York St John

For more information please contact RaY at ray@yorks.ac.uk

Keywords: PBK; TOPK; radiosensitivity; cancer

TOPK modulates tumour-specific radiosensitivity and correlates with recurrence after prostate radiotherapy

Giacomo Pirovano¹, Thomas M Ashton¹, Katharine J Herbert¹, Richard J Bryant^{1,2}, Clare L Verrill², Lucia Cerundolo², Francesca M Buffa¹, Remko Prevo¹, Iona Harrap¹, Anderson J Ryan¹, Valentine Macaulay¹, William G McKenna¹ and Geoff S Higgins^{*1}

¹CRUK/MRC Oxford Institute for Radiation Oncology, University of Oxford, Old Road Campus Research Building, Roosevelt Drive, Oxford OX3 7DQ, UK and ²Nuffield Department of Surgical Sciences, Oxford Cancer Research Centre, University of Oxford, Old Road Campus Research Building, Roosevelt Drive, Oxford OX3 7DQ, UK

Background: Tumour-specific radiosensitising treatments may enhance the efficacy of radiotherapy without exacerbating side effects. In this study we determined the radiation response following depletion or inhibition of TOPK, a mitogen-activated protein kinase kinase family Ser/Thr protein kinase that is upregulated in many cancers.

Methods: Radiation response was studied in a wide range of cancer cell lines and normal cells using colony formation assays. The effect on cell cycle progression was assessed and the relationship between TOPK expression and therapeutic efficacy was studied in a cohort of 128 prostate cancer patients treated with radical radiotherapy.

Results: TOPK knockdown did not alter radiation response in normal tissues, but significantly enhanced radiosensitivity in cancer cells. This result was recapitulated in TOPK knockout cells and with the TOPK inhibitor, OTS964. TOPK depletion altered the G₁/S transition and G₂/M arrest in response to radiation. Furthermore, TOPK depletion increased chromosomal aberrations, multinucleation and apoptotic cell death after irradiation. These results suggest a possible role for TOPK in the radiation-induced DNA damage checkpoints. These findings have clinical relevance, as elevated TOPK protein expression was associated with poorer clinical outcomes in prostate cancer patients treated with radical radiotherapy.

Conclusions: This study demonstrates that TOPK disruption may cause tumour-specific radiosensitisation in multiple different tumour types.

Radiotherapy has a major role in cancer treatment. Increasing ionising radiation (IR) dose may improve the probability of local tumour control but increases the risk of damage to the surrounding healthy tissue. The ‘therapeutic window’ is the range of radiation doses that can be delivered to patients with limited side effects.

Intrinsic radiosensitivity gives rise to differences in susceptibility to ionising radiation (IR) treatment and impacts on clinical endpoints, including survival, local control and disease-free survival (Hanahan and Weinberg, 2011). Our laboratory developed a high-throughput colony formation assay (CFA) and screened an

siRNA library of 709 protein kinases (Tiwana *et al*, 2015), which identified T-LAK cell-originated protein kinase, TOPK (also known as PDZ-binding kinase) as a highly ranked radiosensitising gene. We chose to further investigate TOPK as a potential target to widen the therapeutic window due to its differential expression between cancer and normal tissues.

TOPK is a Ser/Thr protein kinase of 322 amino acids first identified from a lymphokine-activated killer T-cell subtraction cDNA fragment library (Abe *et al*, 2000) and as a physical interactor of the hDlg tumour suppressor protein (Gaudet *et al*, 2000).

*Correspondence: Dr GS Higgins; E-mail: geoffrey.higgins@oncology.ox.ac.uk

Revised 10 May 2017; accepted 2 June 2017; published online 4 July 2017



TOPK is a member of the mitogen-activated protein kinase kinase family involved in growth, migration and mitotic progression (Abe *et al*, 2000; Gaudet *et al*, 2000; Matsumoto *et al*, 2004; Shih *et al*, 2012; Shinde *et al*, 2013; Park *et al*, 2006). TOPK activity is regulated by CDK1/cyclin B-mediated phosphorylation at its Thr9 residue, which promotes mitotic entry at the G₂/M checkpoint (Abe *et al*, 2000; Gaudet *et al*, 2000; Matsumoto *et al*, 2004). TOPK inhibits PTEN, leading to AKT/PI3K activation (Shih *et al*, 2012; Shinde *et al*, 2013). During mitosis, TOPK phosphorylates histone H3 (Ser10) during the transition from prophase to metaphase, (Park *et al*, 2006) specifically targets C2H2 zinc finger proteins to promote chromatin dissociation (Rizkallah *et al*, 2015) and complexes with cyclin B/CDK1 to phosphorylate PRC1 and promote chromosomal separation and cytokinesis (Abe *et al*, 2007). TOPK depletion results in cytokinetic failure and cell cycle arrest, (Abe *et al*, 2007; Park *et al*, 2010), which leads to multinucleation in HeLa cells (Matsumoto *et al*, 2004). TOPK directly inhibits the tumour-suppressor p53 with subsequent downregulation of p21 expression and impaired regulatory control over cellular growth (Zykova *et al*, 2010).

TOPK is involved in the cellular response to doxorubicin (Nandi *et al*, 2007; Zykova *et al*, 2010), arsenite (As³⁺) (Zykova *et al*, 2006) and ultraviolet radiation (Ayllon and O'Connor, 2007), but has not been studied in the context of IR. Overexpression of TOPK in HT1080 cells following doxorubicin treatment suppresses G₂/M checkpoint control, leading to premature mitotic entry and polyploidy (Nandi *et al*, 2007). Furthermore, TOPK co-localises with γ -H2AX foci after arsenite treatment and inhibits apoptosis in RPMI-7951 cells (Zykova *et al*, 2006), and TOPK depletion reduces the number of γ -H2AX foci in MCF-7 cells following UV-induced DNA damage (Ayllon and O'Connor, 2007).

TOPK expression is upregulated in most cancers (Rhodes *et al*, 2007); however, expression is restricted in normal tissues to a few organs such as testis and placenta (Abe *et al*, 2000; Gaudet *et al*, 2000; Matsumoto *et al*, 2004; Fujibuchi *et al*, 2005). High TOPK expression has been associated with adverse effects on local tumour control in non-small-cell lung cancer and with mutant p53 expression levels (Lei *et al*, 2013; Shih *et al*, 2012; Lei *et al*, 2015). Similarly, high TOPK expression correlates with worse overall survival and recurrence-free survival in breast, gastric and colorectal cancer (O'Leary *et al*, 2013; Xiao *et al*, 2015; Ohashi *et al*, 2017). In colorectal cancer, increased levels of TOPK are correlated with high levels of interleukin-8 (Xiao *et al*, 2015) and with oncogenic KRAS and BRAF mutations (Zlobec *et al*, 2010). In prostate cancer, high TOPK expression correlates with increased invasiveness and cancer stage (Sun *et al*, 2015). Conversely, low TOPK expression is predictive of poor prognosis in cholangiocarcinoma patients (He *et al*, 2010).

In the present study we report a novel role for TOPK as a tumour-specific modulator of radiosensitivity. TOPK has the potential to be exploited as a clinical radiosensitiser due to its differential expression between cancer and normal tissues. TOPK depletion impairs G₂/M checkpoint activation and increases chromosomal aberrations, apoptosis and multinucleation. Elevated TOPK protein expression is associated with poorer clinical outcomes in a cohort of prostate cancer patients treated with radical radiotherapy.

MATERIALS AND METHODS

Cell culture. HCT116, HeLa, MRC5, HFL-1, DU145, PC3, H1299 and T24 cell lines were purchased from American Type Culture Collection (ATCC, Manassas, VA, USA). SQ2OB cells were provided by Dr Ralph Weichselbaum (University of Chicago, Chicago, IL, USA). T24 cells were maintained in RPMI-1640,

MRC5 cells in MEM and HFL-1 cells in DMEM/F-12 Ham's. The HAP1 cell lines were purchased from Horizon Discovery (Cambridge, UK) and maintained in IMDM medium. HAP1 is a near-haploid human cell line derived from chronic myelogenous leukaemia cell line. HAP1 cells are adherent with fibroblast-like morphology. TOPK knockout was achieved via Crispr/Cas9 editing to contain a 4 bp deletion in the coding exon of TOPK. HUVEC and HMEC_1 cells were maintained in EBM-Plus (Lonza, Walkersville, MD, USA) medium. All other cells were maintained in DMEM. All cells were maintained with 10% FBS and all medium was purchased from Sigma (St Louis, MI, USA). All cell lines were authenticated by LGC standards (ATCC) by short tandem repeat profiling and tested for mycoplasma using MycoAlert (Lonza).

siRNA transfection. Reverse-transfection protocol was used (final concentration 20 nM) using Ambion Silencer Select siRNA (Life Technologies) INTERFERin-HTS (Polyplus) transfection reagent as previously described (Tiwana *et al*, 2015). siTOPK: 5'-GACUAAUGGAUGAAGCUAAtt-3'; siTOPK_2: 5'-CCCU-GAGGCUUGUACAUAUtt-3'; siTOPK_3: 5'-GCACUAAUGAA-GACCCUAAAtt-3'.

Cell synchronisation. Cell synchronisation in G₁/S phase was achieved using 2 mM thymidine block for 18 h, followed by 9 h release in fresh medium and then 14 h further incubation with 2 mM thymidine. Cells were released in fresh medium after two washes in PBS.

Immunoblotting. Protein lysates were prepared using RIPA lysis buffer (Thermo Scientific, Rockford, IL, USA) with protease inhibitors (Roche, Mannheim, Germany) and phosphatase inhibitors (Sigma). Protein concentration was determined using the BCA assay (Thermo Scientific). Bound antibodies were detected by developing film from nitrocellulose membranes exposed to chemiluminescence reagent (Immobilon Western Chemiluminescent Substrate, EMD Millipore, Merck KGaA, Darmstadt, Germany).

Antibodies. The following antibodies were used: anti-TOPK for immunoblotting (Sigma SAB5300406 clone 2C8, 1:1000); anti-TOPK for immunohistochemistry (Cell Signaling Technology, Danvers, MA, USA 4942, 1:100); anti-TOPK (phospho T9) antibody (Abcam, Cambridge Science Park, Cambridge, UK ab184953, 1:1000); anti-cyclin E1 (Cell Signaling Technology 4129, 1:1000); anti-cyclin B1 (Cell Signaling Technology 4138, 1:1000); anti-phospho-CDK1 (Tyr15) (Cell Signaling Technology 4539, 1:1000); anti-CDK1 (Cell Signaling Technology 9116, 1:1000); anti-phospho histone H3 (Ser10) (Cell Signaling Technology 3377, 1:1000); anti-histone H3 (Cell Signaling Technology 9715, 1:1000); anti-Akt (Cell Signaling Technology 9272S, 1:1000); anti-phospho-Akt (Cell Signaling Technology 4060S, 1:1000); anti-Vinculin (Abcam ab18058, 1:40 000); and anti- γ -H2AX Ser139 (Upstate/Millipore, 05-636, Temecula, CA, USA).

Colony formation and viability assays. Inhibitor-treated and siRNA-transfected CFAs were performed and analysed as previously described (Tiwana *et al*, 2015). To determine the effect of OTS964 on cell viability, resazurin was added to the cells for 3 h after 72 h drug treatment. Fluorescence was measured using a POLARstar OMEGA plate reader (BMG Labtech, Ortenberg, Germany). IC₅₀ was calculated from non-linear curve fitting of Log[Inhibitor] vs Response using variable slope (four parameters; GraphPad Prism Software v 7.0c, San Diego, CA, USA).

Flow cytometry. Bromodeoxyuridine (BrdU) (20 μ M; Sigma) was added to adherent cells 30 min before fixing. Cells were fixed in ice-cold 70% ethanol, incubated at room temperature with 2 M HCl containing 0.1 mg ml⁻¹ pepsin for 20 min and resuspended in

100 μ l of 2% FBS/1 \times PBS with 1 μ l mouse anti-BrdU monoclonal antibody (1:100, BD Bioscience, San Jose, CA, USA) for 90 min. Samples were resuspended in 100 μ l 2% FBS/1 \times PBS with 0.5 μ l Goat anti-Mouse AF488 antibody (Life Technologies, Eugene, OR, USA) for 60 min in the dark. Samples were washed in PBS and resuspended in 0.5 ml PBS containing 50 μ g ml⁻¹ propidium iodide (PI). Samples were analysed using FACSsort cytometer (Becton Dickinson, San Jose, CA, USA).

Microscopy. For live cell analysis, cells were stably transfected with the pH2B_mCherry_IRES_puro2 plasmid (Steigemann *et al*, 2009) (from Daniel Gerlich, Addgene plasmid 21045). Phase-contrast and fluorescence images were taken every 30 min for 48 h, with cells maintained at 5% CO₂, 37 °C. For fixed cell analysis, cells were plated onto glass coverslips, fixed with 70% ice-cold methanol for 10 min and then incubated with PBS containing 1 μ g ml⁻¹ DAPI and 1 μ g ml⁻¹ FITC. Coverslips were then washed and mounted on a microscope slide using antifade medium Vectashield (Burlingame, CA, USA). Samples were analysed with a confocal microscope (Zeiss710, Zeiss, Oberkochen, Germany) and cell morphology was scored manually using ImageJ open source software. Mitotic chromosomes were captured by incubating the cells in colcemid (30 ng ml⁻¹) for 1 h and metaphase nuclei prepared by incubating samples in hypotonic solution (75 mM KCl) for 30 min before fixation in Carnoy solution (3:1 methanol:glacial acetic acid). Chromosome suspensions were dropped onto slides and mounted using Vectashield with DAPI. Samples were imaged with \times 100 oil-immersion lens using a Nikon 90i confocal microscope (Nikon, Minato, Tokyo, Japan).

Patient samples. Prostate cancer samples and associated anonymous follow up data (ORB ethics 09/H0606/5 + 5) included 128 patients who received radical radiotherapy with curative intent. All patients that participated in the study and whose samples were used for analysis provided informed signed consent. Prostate biopsies were collected at the time of diagnosis. External beam radiotherapy was 3D conformal CT planned. A 55 Gy dose was typically delivered to the planned target volume in 20 fractions over a 4-week period with neoadjuvant and concurrent androgen deprivation therapy. Assuming an α/β ratio for prostate cancer of 1.8 Gy (Dearnaley *et al*, 2016), this dose/fractionation schedule is equivalent to 65.9 Gy in 2 Gy fractions. All patients were treated at the Oxford Cancer Centre and human tissue was used with National Research Ethics approval (study 07/H0606/120).

Immunohistochemistry. Sections were de-paraffinised in histoclear and rehydrated through graded ethanol to water. Endogenous peroxidase activity was inactivated using 3% H₂O₂ in methanol. Sections were blocked with 5% normal goat serum and incubated with primary antibody at 4 °C overnight. A biotinylated secondary antibody was added for 45 min followed by an avidin/biotin-based peroxidase solution and incubated with 3,3'-diaminobenzidine solution before counterstaining with haematoxylin. All sections were dehydrated using increasing percentages of ethanol followed by histoclear and mounted in omnimount medium.

Scoring and statistical analysis. Patient samples were assigned a blind intensity score ranging from 0 (no expression) to 3 (maximal expression) multiplied by the percentage of stained cells (total TOPK expression score, 0–600). For univariate analysis, data were initially binarised as described in the text, whereas significance was assessed using the log-rank test. Cox survival analysis was performed. Analyses were done using SPSS statistic 22 software (UNICOM Global, Mission Hills, CA, USA). All statistical tests were performed as two-tailed tests and differences were considered significant at a *P*-value of less than 0.05. All assay data are representative of three independent experiments and are presented as mean \pm s.d. from triplicate wells, unless otherwise stated (**P* < 0.05, ***P* < 0.01 and ****P* < 0.001). Survival curves were fitted

using nonlinear regression and were analysed by factorial two-way ANOVA, with interaction term significance of *P* < 0.05.

RESULTS

TOPK is a tumour-specific novel modulator of radiosensitivity.

The impact of TOPK knockdown on radiosensitivity was investigated in a panel of cancer cell lines using a CFA. Transient knockdown of TOPK was achieved by siRNA transfection at a final concentration of 20 nM (siTOPK), with non-targeting siRNA (siNT) used as a control. Radiosensitisation was observed in all siRNA treated cancer cell lines, with the survival enhancement ratio at a SER₁₀ of 1.28 (*P* = 0.007) in HeLa cells (cervical), 1.45 (*P* = 0.002) in HCT116 cells (colorectal), 1.55 (*P* = 0.005) in DU145 cells (prostate) and 1.45 (*P* < 0.001) in HAP1 TOPK CRISPR/Cas9 knockout cells (Figure 1A). Four other cancer cell lines showed similar enhancement ratios: 1.37 (*P* = 0.006) in T24 cells (bladder), 1.28 (*P* = 0.003) in H1299 cells (lung), 1.13 (*P* < 0.001) in SQ20B cells (head and neck) and 1.35 (*P* = 0.004) in PC3 cells (prostate; Supplementary Figure 1A).

The Oncomine 3.0 database revealed that TOPK expression is predominantly limited to cancer tissues, with many studies showing high TOPK expression in tumour types including the brain, breast and lung (Supplementary Figure 1B; Rhodes *et al*, 2007). This is in accordance with the undetectable TOPK expression in MRC5 and HFL-1 normal lung fibroblasts (Supplementary Figure 1C). Correspondingly, no significant radiosensitisation was observed in HFL-1 or MRC5 cells, suggesting that the observed radiosensitising effect is tumour specific (Figure 1B). Two additional TOPK siRNAs were used in HCT116 cells to confirm that the radiosensitisation was not due to an off-target effect (Supplementary Figure 1D). To examine the effect of TOPK overexpression on colony formation in HCT116 cells, a CFA was performed, which did not affect radiosensitisation when compared to the empty vector control (Supplementary Figure 1E), suggesting potential differences between endogenous and exogenous TOPK expression or the presence of a radio-resistance threshold that is not altered by further increase in TOPK levels.

OTS964 is a small molecular compound previously shown to inhibit TOPK kinase activity (Matsuo *et al*, 2014). In order to study the effect of OTS964 on cell viability, the IC₅₀ was determined for a panel of cell lines treated with the inhibitor for 72 h. In HAP1 WT and HAP1 TOPK cell lines, the IC₅₀ was 83 nM and 567 nM, respectively (Supplementary Figure 1F). In addition, the IC₅₀ was greater in HFL1 and MRC5 cells than any of the tested cancer cell lines, indicating that cells with high TOPK expression are most sensitive to the inhibitor (Supplementary Figure 2A). We next investigated whether treatment with OTS964 could elicit tumour-specific radiosensitisation comparable to siRNA-mediated TOPK depletion. Treatment of nocodazole-arrested HCT116 cells with 100 nM or 200 nM OTS964 for 4 h is sufficient to inhibit the TOPK substrate motif, HpTGEKP, indicating that TOPK is inhibited under these conditions (Supplementary Figure 2B). Cell lines with an IC₅₀ of 60 nM or less were treated with 70–100 nM OTS964 and those with an IC₅₀ above 60 nM were treated with 200 nM OTS964. The inhibitor was added 4 h before IR and washed off 24 h after IR. The tested cancer cell lines were radiosensitised (Figure 1C and Supplementary Figure 2C) with SER₁₀ values of 2.14 (*P* < 0.001) in HeLa, 1.40 (*P* < 0.001) in HCT116, 1.42 (*P* < 0.001) in DU145, 3.02 (*P* < 0.001) in T24, 1.33 (*P* < 0.001) in H1299, 1.54 (*P* = 0.003) in SQ20B and 1.34 (*P* < 0.001) in PC3. The normal cell lines tested were not radiosensitised, with SER₁₀ of 0.90 (*P* = 0.172) in HFL-1, 1.08 (*P* = 0.601) in MRC5 (Figure 1D), 1.04 (*P* = 0.817) in HUVEC (umbilical vein epithelium) and 1.00 (*P* = 0.466) in HMEC_1

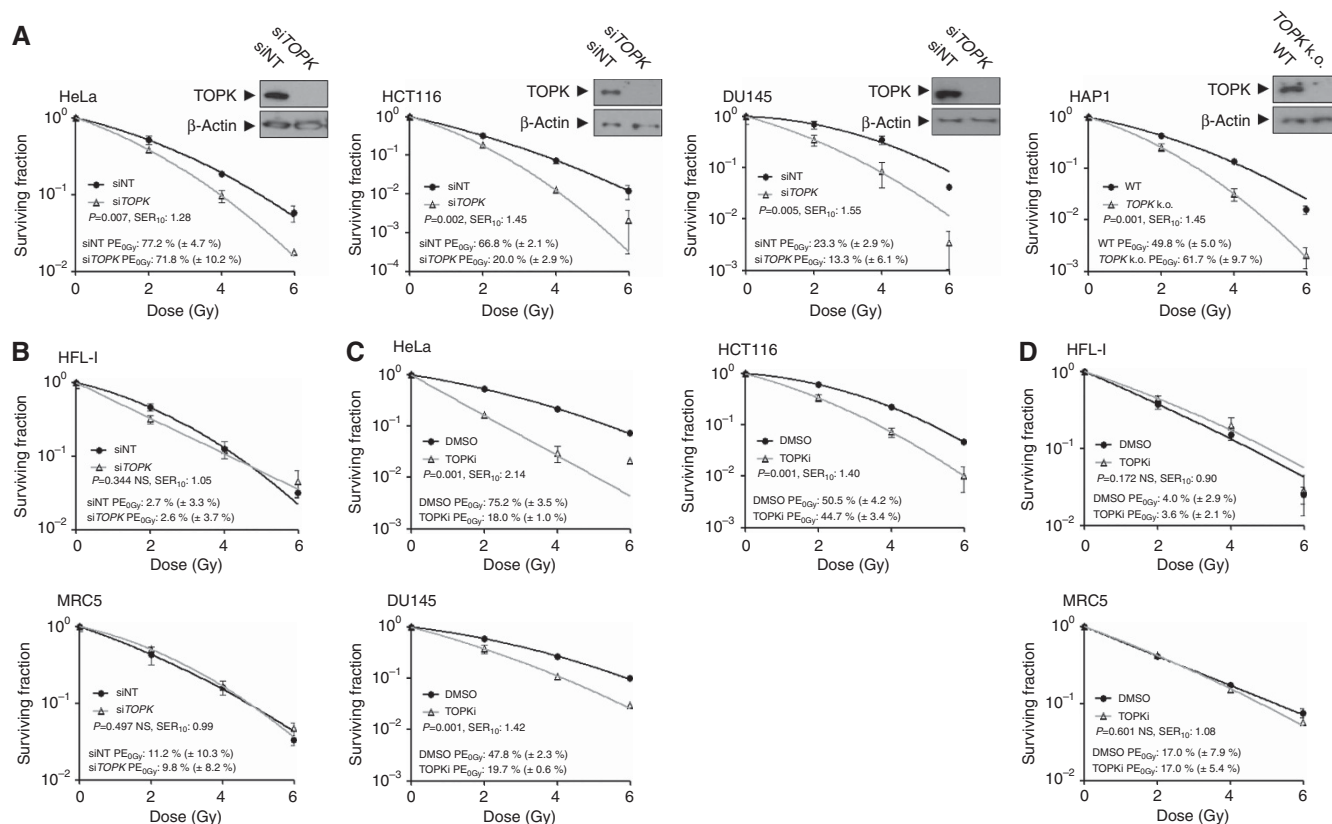


Figure 1. TOPK is a tumour-specific modulator of radiosensitivity. (A) TOPK was transiently knocked down with siRNA (siTOPK) and post-irradiation clonogenic survival was assessed in cancer-derived cells. Transfection with siNT was used as a control and knockdown efficiency was confirmed by immunoblotting (insets). (B) No significant TOPK-dependent radiosensitisation was detected in HFL-1 and MRC5 cells. (C) TOPK activity was inhibited by 4 h pretreatment with 70–200 nM OTS964 (70 nM for HCT116, DU145, 100 nM for HeLa, 200 nM for HFL-1, MRC5). (D) No significant TOPK-dependent radiosensitisation was detected in HFL-1 and MRC5 cells treated with OTS964. All data are representative of three independent experiments and are presented as mean \pm s.d. from triplicate wells. Survival curves were fitted using non-linear regression. Results were analysed by factorial two-way ANOVA, with interaction term significance of $P < 0.05$. PE = plating efficiency; SER₁₀ = survival enhancement ratio at a surviving fraction of 0.10.

(microvascular epithelium) Supplementary Figure 2D. These experiments suggest that TOPK knockdown or kinase inhibition induces tumour-specific radiosensitisation with minimal effects on normal tissue cells.

TOPK depletion alters cell cycle progression following IR. In order to investigate the role of TOPK in the cellular response to IR, a time-course experiment was conducted to determine cell cycle progression of HCT116 cells after 4 Gy IR. Asynchronous cells were irradiated 72 h post siRNA transfection. Cell cycle stage was assessed by flow cytometry analysis using anti-BrdU and PI staining. At 0 h, TOPK depletion caused only slight changes in cell cycle distribution, with a 5% increase in the G₁ fraction compared to the control, and 3 and 2% decreases in the early S and G₂/M fractions, respectively (Figure 2A, quantified in Supplementary Table 1). At 2 h after IR, a 12% increase in the siTOPK G₁ population and corresponding decreases of 4 and 3% in the early S, late S and G₂/M populations, respectively, were observed. The biggest differences were detected at 8 h post IR, with siTOPK cells showing an 18% increase in G₁ phase, a 5% decrease in late S and a 14% decrease in G₂/M compared with siNT.

The observed increase in G₁ and corresponding decrease in G₂/M following IR in TOPK-depleted cells could be due to delay in G₁ exit, premature mitotic entry, increased cycling rate or a combination of these factors. To distinguish between these possibilities, TOPK-depleted HCT116 cells were synchronised in G₁ via double-thymidine block, irradiated at 4 Gy and immediately

released into fresh culture medium (Figure 2B and Supplementary Table 2). Exit from G₁ into S-phase was delayed in cells depleted of TOPK when compared with the control (72% decrease in the G₁ population after 2 h for the control cells, but only a 46% decrease in the G₁ population after 2 h for the cells depleted of TOPK compared to 0 h). Delayed G₁ exit in the TOPK knockdown cells was independent of IR (Figure 2B). The G₁ population in the cells depleted of TOPK was nearly triple that of the control at 8 h after release. Correspondingly, there was delayed entry into S phase in irradiated TOPK-depleted cells, with a peak in early S phase at 4 h of only 29%, compared to a higher peak of 48% at 2 h in the control cells. The peak in late S phase was at 8 h for both treatments, but was 45% in the TOPK-depleted cells compared with 66% in the control cells. Cell cycle distribution was comparable at the 24 h time point in the presence or absence of IR for all treatments. These findings are consistent with a delay in G₁ exit following TOPK depletion.

Markers for cell cycle regulation (cyclin B1 and E1, CDK1 and phospho-CDK1) and mitosis (phosphorylation of histone H3 at Ser₁₀) were assessed in G₁ synchronised HCT116 cells and are presented in Figure 2C and Supplementary Figure 3A. TOPK phosphorylation peaked at 8 h post release in the control cells (Figure 2C). Levels of CDK1 peaked between 6 and 10 h in both the control and TOPK-depleted cells. However, CDK1 phosphorylation (Tyr15) was much reduced in the TOPK-depleted cells, indicating a possible impairment of G₂/M checkpoint in these cells. Expression of the mitotic markers phospho-histone H3 and cyclin

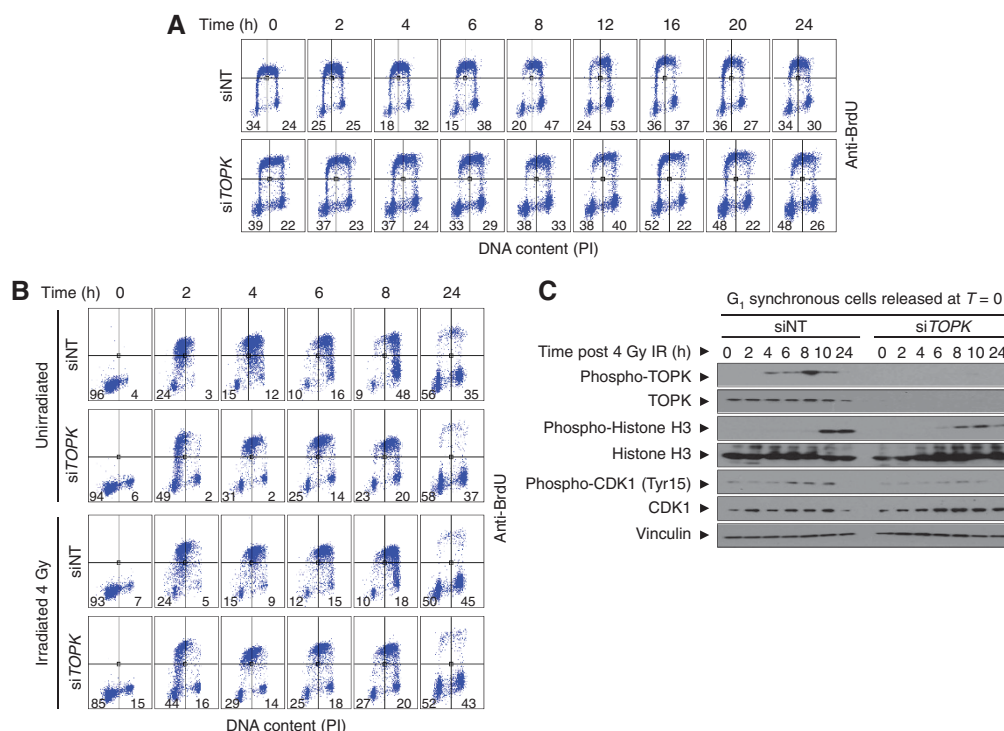


Figure 2. TOPK depletion alters cell cycle progression following IR. Bromodeoxyuridine (BrdU) was added to cells 30 min before fixation and cell cycle stage was assessed by flow cytometry analysis using anti-BrdU and PI staining. The impact of TOPK depletion by siRNA on cell cycle progression was assessed in asynchronous HCT116 cells (**A**) and in HCT116 cells released from double thymidine block (**B**) following 4 Gy irradiation at $T=0$. Numbers indicate the percentage G₁ population (PI –/BrdU –, lower left quadrant) or G₂/M population (PI +/BrdU –, lower right quadrant). Early S (BrdU +/PI –, top left quadrant). Late S (BrdU +/PI +, top right quadrant). (**C**) Immunoblotting was used to assess the effect of TOPK knockdown on the expression of cell cycle proteins in samples from the experiment described in (**B**). Vinculin was used as a loading control. Data displayed are representative of three independent repeats.

B1 peaked at 10 h post-release in the control cells, reflecting a coordinated progression into mitosis (Figure 2C and Supplementary Figure 3A). In contrast, post-release mitotic entry occurred earlier for cells depleted of TOPK, with H3 phosphorylation and cyclin B1 expression occurring earlier at 6–8 h post release, despite the delayed G₁ exit (Figure 2C). Cyclin E1 expression confirmed enrichment of G₁/early S phase cells at the earliest time points ($T=0$ and $T=2$) in the control sample, decreasing post release and reappearing at the latest time point ($T=24$), indicating a return to G₁. However, cyclin E levels did not decrease as rapidly in the TOPK-depleted cells, consistent with a delay in G₁ exit. TOPK has been previously shown to have a role in the PI3K/Akt pathway (Ayllon and O'Connor, 2007), the levels of phospho-Akt were therefore investigated after IR and did not show a significant dependency on the levels of TOPK (Supplementary Figure 3B). These results are consistent with both a delay in G₁ exit and an impaired G₂/M transition in TOPK-depleted cells.

TOPK depletion promotes multinucleation and apoptosis after IR. Altered cell cycle progression and failure to activate DNA damage checkpoints can result in chromosomal aberrations, mitotic catastrophe, micronucleation, multinucleation and apoptosis (Dillon *et al.*, 2014; Visconti *et al.*, 2016). To determine the consequences of altered cell cycle progression and G₂/M arrest in TOPK-depleted cells, we performed live-cell imaging using HCT116 H2B-mCherry cells. The cells were transfected with siNT or siTOPK, and after 72 h were exposed to 4 Gy IR. Cells were then imaged every 30 min for 48 h. The fate of 50 cells was determined for each experimental replicate and transitions through mitosis and interphase were recorded (Figure 3A and Supplementary Movies 1–4). There was no significant difference in the length of mitosis, as

the first mitosis was 1.9 h in the control cells compared to 1.5 h in the TOPK-depleted cells ($P=0.231$). However, in TOPK-depleted cells there was a significant 8% increase ($P=0.024$) in the number of cells that entered mitosis, attempted cell division and then became multinuclear during the first division (Figure 3B). Furthermore, a nonsignificant 3% increase in apoptosis was observed in TOPK-depleted cells before the first mitosis ($P=0.705$) and a significant 14% increase in apoptosis was observed in the daughter cells prior to the second mitosis ($P=0.001$).

To fully evaluate the impact of this finding at later time-points, we quantified irradiation-induced multinucleation in fixed HCT116 cells following TOPK knockdown using DAPI and FITC as nuclear and cytoplasmic stain. TOPK knockdown resulted in a significantly higher number of multinucleated cells ($P<0.01$) following irradiation, but no differences were observed in unirradiated cells (Figure 3C). To further investigate the increase in apoptosis in irradiated TOPK-depleted cells, Hoechst and Annexin V assays were used to monitor apoptotic cell death at 24, 48 and 72 h after 4 Gy IR. In both cases, TOPK knockdown caused a significant increase in the percentage of apoptotic cells at the latest time points compared to the siNT control (Figure 3D, Supplementary Figure 3C and Supplementary Table 3). The same result was reproducible using siTOPK_2 and siTOPK_3 siRNAs for the Hoechst assay (Supplementary Figure 3D). Taken together, these data suggest that irradiation of TOPK-depleted cells results in post-mitotic chromosomal instability, multinucleation and ultimately apoptotic cell death.

TOPK depletion causes chromosomal aberrations in response to IR. In order to test whether TOPK-dependent radiosensitisation

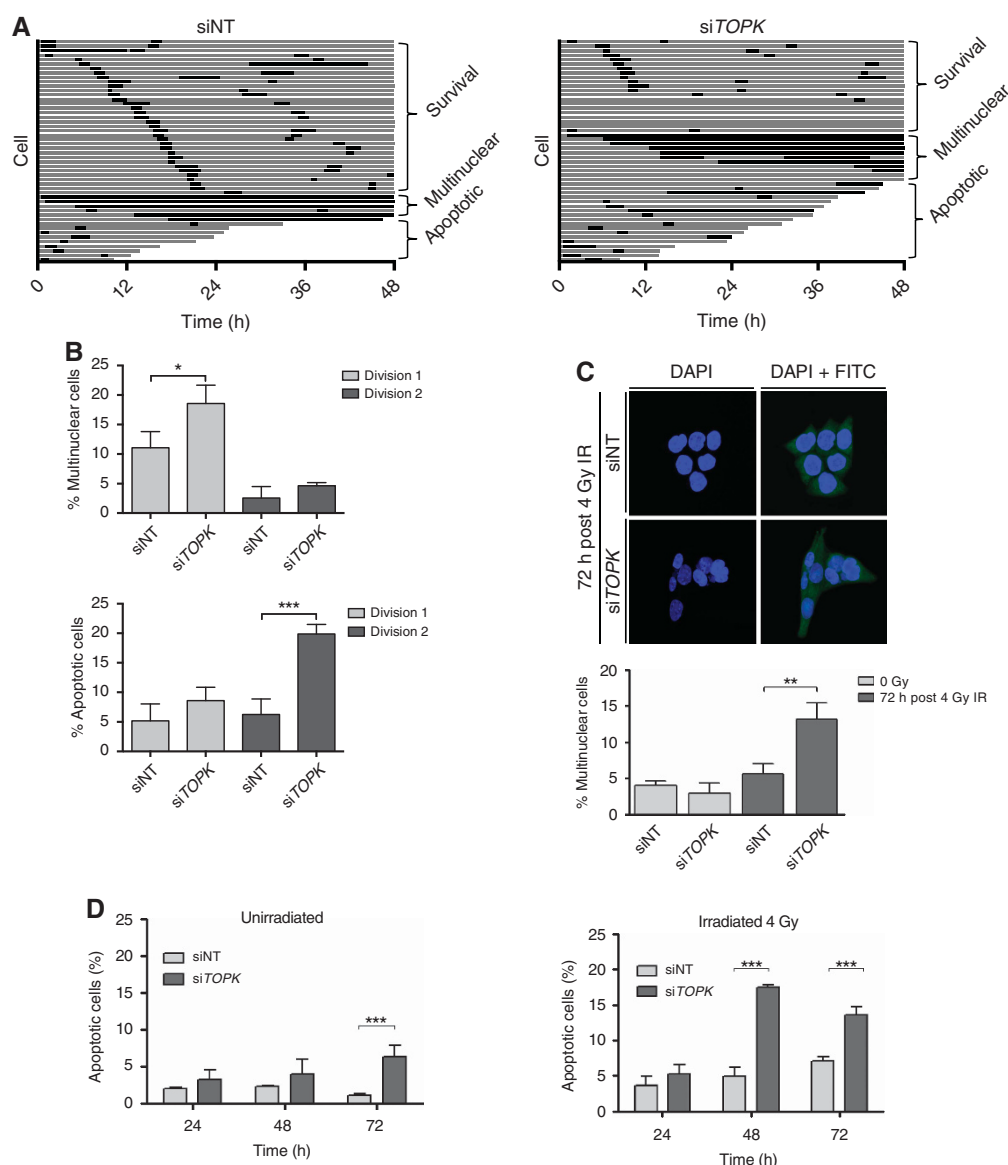


Figure 3. *TOPK* depletion causes multinucleation and apoptosis in HCT116 cells. Cells were irradiated 72 h post siRNA treatment. **(A)** Live-cell imaging following the fate of 50 HCT116 H2B-mCherry cells for 48 h after 4 Gy IR. Each horizontal bar represents one cell, with interphase shown in grey and mitosis shown in black. Following division, the first daughter cell to undergo division, apoptosis or multinucleation is shown. **(B)** The percentage of cells that apoptosed or became multinuclear during the first or second cell divisions after IR ($n=3$, average of 3 replicates). **(C)** Analysis of IR-induced multinucleation in fixed HCT116 treated cells 72 h after 4 Gy IR. At least 100 cells were counted per condition. Nuclei were stained with the DAPI DNA stain (blue) and FITC was used as a cytoplasmic counterstain (green). **(D)** Cell death in the presence (right panel) and absence (left panel) of 4 Gy irradiation was assessed with Hoechst staining to identify bright apoptotic nuclei in cells transfected with NT or *TOPK* siRNA and irradiated with 4 Gy at $T=0$. Data displayed are representative of three independent experiments and were analysed using unpaired two-sided *t*-tests; * $P<0.05$, ** $P<0.01$ and *** $P<0.001$.

was due to erroneous DNA repair, post-IR DNA damage was compared in *TOPK* knockdown cells and control cells using an alkaline Comet assay. No differences in DNA damage were detected at 30 min, 2 or 8 h after 4 Gy IR (Supplementary Figure 3E). The kinetics of γ -H2AX foci formation and resolution was then assessed after 4 Gy IR. Although a small statistically significant decrease in the number of foci was identified in *TOPK*-depleted cells at 30 min post IR, this was not observed at 4, 8 and 24 h post IR (Supplementary Figure 3F). These results suggest that *TOPK* does not affect double strand break (DSB) repair.

To investigate whether *TOPK* knockdown could induce mitotic progression errors, metaphase spreads were prepared in HCT116

cells with siNT or si*TOPK* knockdown and the number of aberrations present per genome were quantified at 24, 48 and 72 h after 4 Gy IR (Figure 4A). Chromosomal aberrations such as breaks, exchanges and fragmentation were significantly greater in *TOPK*-depleted cells when compared with the control at all time points (Figure 4B).

TOPK levels affect survival in prostate cancer patients after radiotherapy. To examine the clinical relevance of our findings, the relationship between *TOPK* expression and therapeutic efficacy was studied in a cohort of 128 prostate cancer patients treated with radical radiotherapy. Over a median (interquartile range) follow-up period of 7.7 (6.9–8.4) years following radical radiotherapy,

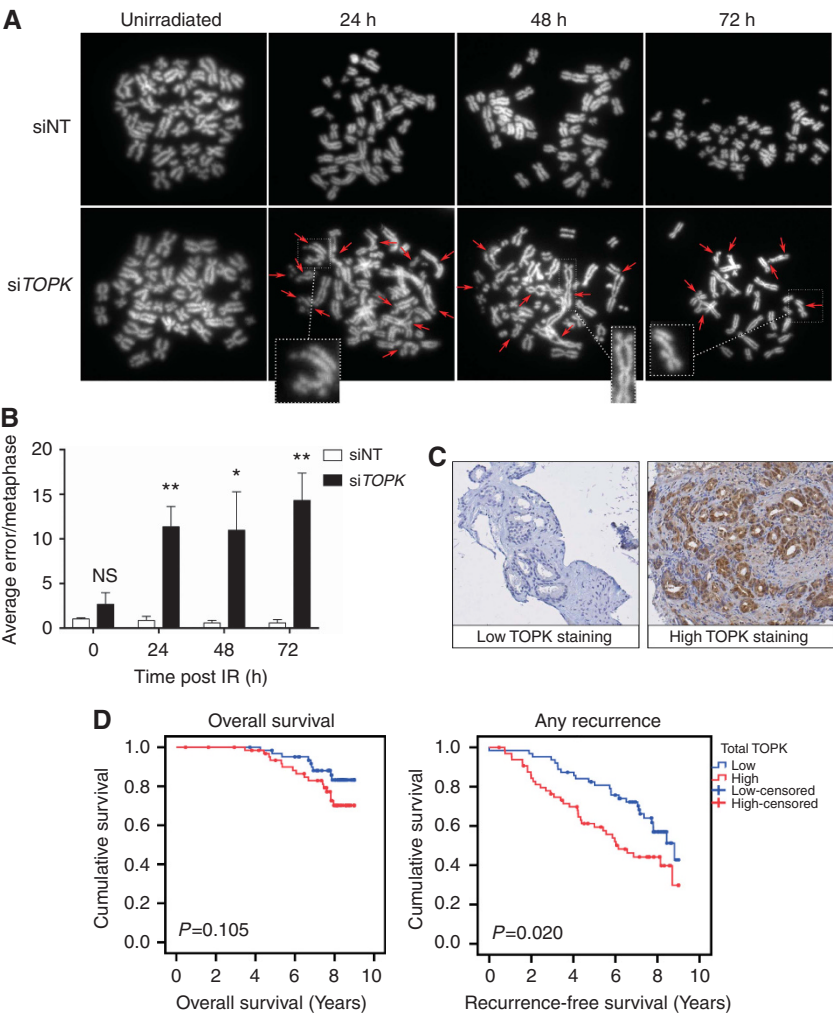


Figure 4. High TOPK expression correlates with poor outcomes in prostate cancer patients. **(A)** HCT116 cells were transfected with siRNA and irradiated (4 Gy). Metaphases were collected at 24, 48 and 72 h following irradiation and scored for chromosomal aberrations, with 40 nuclei analysed in each group. Images of representative metaphases include examples of typical errors detected (insets). Arrows indicate chromosomal aberrations. **(B)** Average number of errors per metaphase from three independent experiments * $P<0.05$ and ** $P<0.01$. **(C)** Representative photomicrographs taken following immunohistochemistry staining with an anti-TOPK antibody, showing non-staining in disease-free prostate epithelium and strong nuclear and cytoplasmic TOPK expression in prostatic carcinoma. **(D)** Kaplan–Meier analysis of TOPK expression and overall survival, and any recurrence in prostate cancer patients following radical radiotherapy ($n=128$). P -value from univariate analysis.

Table 1. Diagnostic biopsy pathology characteristics of 128 prostate cancer patients at baseline	
Category	N (%)
Pre-treatment PSA	
≤ 10	46 (35.9)
10.1–20	43 (33.6)
≥ 20	32 (25)
Unknown	7
Clinical T stage	
≤ 2	78 (60.9)
≥ 3	42 (32.8)
Unknown	8 (6.3)
Gleason grade	
≤ 6	30 (23.4)
7	83 (64.9)
≥ 8	15 (11.7)

Abbreviation: PSA = prostate specific antigen.

Table 2. Multivariate analysis of clinical prognostic factors for the development of prostate cancer recurrence and any-cause death				
	Any recurrence		Any-cause death	
	HR (95% CI)	P	HR (95% CI)	P
All prostate cancer cases				
cT stage	1.33 (0.77–2.3)	0.3	0.63 (0.26–1.56)	0.32
PSA	1.07 (0.77–1.48)	0.7	0.86 (0.51–1.46)	0.58
Primary Gleason ≥ 4	1.72 (1.01–2.93)	0.048	2.2 (0.93–5.2)	0.07
Total TOPK	1.73 (1.02–2.92)	0.04	1.65 (0.72–3.8)	0.24

Abbreviations: CI = confidence interval; HR = hazard ratio; PSA = prostate specific antigen.

prostate cancer had recurred in 62/128 (48%) patients, of whom 44/128 (34%) had non-metastatic recurrence and 18/128 (14%) had metastatic recurrence. Deaths from any cause during the follow-up period occurred in 26/128 (20%) patients.

Immunohistochemistry was used to measure TOPK expression from archived prostate biopsies taken at diagnosis and results were

analysed with respect to clinical outcomes including recurrence-free survival (RFS) and all-cause mortality. Diagnostic biopsy pathology characteristics of the patient cohort at baseline can be found in Table 1. Samples were ranked according to the levels of TOPK expression and the median of the ranking values was used as a cut-point score for high and low TOPK protein expression (Figure 4C). Multivariate analysis was performed to test whether TOPK expression could be a prognostic factor for post-radiotherapy prostate cancer recurrence as presented in Table 2. High levels of TOPK expression in malignant prostate epithelium in diagnostic prostate biopsies at baseline was significantly associated with a reduced RFS following radical radiotherapy ($P = 0.020$). No significant association was observed between levels of TOPK expression and all-cause mortality (Figure 4D). These results indicate that TOPK levels may affect radiotherapy outcome for prostate cancer, and that analysis of TOPK levels might be clinically useful as a prognostic marker when considering treatment with radiotherapy.

DISCUSSION

TOPK depletion radiosensitised a panel of cancer cell lines derived from lung, prostate, cervical, bladder and laryngeal cancers. This effect was independent of p53 status for the cancer cell lines tested, although most of these cell lines are deficient in p53 (Supplementary Table 4). Radiosensitisation was reproducible with siRNAs targeting multiple *TOPK* sequences and no radiosensitisation was observed in normal cells following *TOPK* knockdown. Comparable results were obtained with the TOPK inhibitor, OTS964. These data indicate that TOPK is a tumour-specific modulator of radiosensitivity.

Depletion of cell cycle regulators can cause radiosensitisation (Ayllon and O'Connor, 2007; Dou *et al*, 2015; Lei *et al*, 2015). In support of this argument, cell cycle regulatory kinases including CDC2, ATM, CDKN2B, CDK5R1 and PLK4 were highly ranked in the screen that identified TOPK (Tiwana *et al*, 2015). Alterations of cell cycle progression in TOPK-depleted cells could be due to delay in G₁ exit, premature mitotic entry, increased cycling rate or a combination of these factors. Correspondingly, TOPK-depleted synchronous cells that were irradiated in G₁ and subsequently released had delayed G₁ exit and an impaired G₂/M transition. This is consistent with previous findings that TOPK ensures proper arrest at the G₂/M checkpoint in unirradiated cells (Abe *et al*, 2000; Gaudet *et al*, 2000; Matsumoto *et al*, 2004). Furthermore, TOPK-depleted cells had increased chromosomal aberrations in metaphase, including DNA breaks, chromatid exchanges and DNA fragmentation after IR. The chromosomal aberrations do not seem to arise from a DNA repair defect in TOPK-depleted cells. We propose that these aberrations arise as a consequence of premature mitotic entry, a phenotype that has been observed in ataxia telangiectasia cells, which are deficient in G₂/M checkpoint activation, but exhibit wild-type levels of chromosomal breaks in G₂ following IR (Terzoudi *et al*, 2005; Deckbar *et al*, 2007). Failure of cells to arrest at the G₂/M checkpoint leads to premature chromatin condensation and conversion of unrepaired DSBs into chromosomal breaks, as DSB repair is suppressed during mitosis (Orthwein *et al*, 2014). It is also possible that the chromosomal aberrations arise partly due to inappropriate transition from prophase to metaphase or the inability of C2H2 zinc finger proteins to dissociate from chromatin, as roles for TOPK in these early mitotic activities have been described previously (Park *et al*, 2006; Rizkallah *et al*, 2015).

The studies of both live and fixed cells suggest that a proportion of TOPK-depleted cells attempt mitosis and then become multinuclear during both the first division and during subsequent divisions up to 72 h after IR. Furthermore, a proportion of TOPK-depleted cells divide at least once and then undergo apoptosis during interphase. It is our conjecture that the increases in multinucleation and apoptosis are the consequences of altered cell cycle progression, failure to activate the G₂/M checkpoint and chromosomal aberrations, causing an increase in radiosensitivity. It is possible that the chromosomal aberrations observed during the first mitosis after IR are inherited by the daughter cells, leading to apoptosis. These findings are consistent with other cell cycle regulation genes that are modulators of radiosensitisation. For example, disruption of the G₂/M checkpoint protein 14-3-3 σ promotes early mitotic entry in response to IR, resulting in mitotic catastrophe and cell death (Andreassen *et al*, 2001; Hanahan and Weinberg, 2011). Inhibition of other DNA damage checkpoint proteins such as CHK1 and Wee1 also radiosensitise p53-deficient cells, leading to premature mitotic entry and apoptosis (Garrett and Collins, 2011). TOPK is phosphorylated at Thr9 in G₂ by cyclin B1/CDK1 to promote mitotic entry and as such is also considered to be a G₂/M checkpoint protein (Abe *et al*, 2000; Gaudet *et al*, 2000; Matsumoto *et al*, 2004). Therefore, it is likely that there is a common mechanism of radiosensitisation following depletion of G₂/M checkpoint proteins, including TOPK.

Previous studies have demonstrated a link between high TOPK expression and poor clinical outcomes in different types of cancer, and that TOPK is expressed at low levels in most normal tissues (Rhodes *et al*, 2007; Lei *et al*, 2013, 2015; Park *et al*, 2014; Xiao *et al*, 2015; Ohashi *et al*, 2017). Therefore there is much interest in TOPK as a potential therapeutic target. Our study shows an increased rate of radiotherapy failure in tumours with elevated TOPK expression at baseline, which implies that TOPK expression is an important factor in tumour radioresistance. However, analysis of tumour samples taken as part of a randomised trial of radiotherapy would be required to definitively confirm TOPK expression as a predictive biomarker. Overall survival did not show any significant correlation with levels of TOPK; however, follow-up data did not distinguish between cancer-specific deaths and all-cause deaths and there were few deaths overall. Therefore, it is not possible to state whether TOPK expression influenced overall prostate cancer-specific survival.

Strong correlations between high levels of TOPK and an advanced grade of cancer, metastasis and invasiveness have previously been identified in prostate cancer patients (Brown-Clay *et al*, 2015; Sun *et al*, 2015). Our results support these investigations, revealing a significant association between high TOPK expression and disease recurrence, and add a further level of therapeutic potential by showing these results in the context of radiotherapy. Encouragingly, our study demonstrates that inhibition of TOPK activity is a sensitive and tumour-specific means for enhancing radiosensitivity. As such, the development of small molecule compounds directed against TOPK, such as OTS964, may be a future strategy for enhancing the efficacy of radiotherapy treatment in prostate cancer patients.

ACKNOWLEDGEMENTS

We thank Graham Brown and Mick Woodcock for technical assistance. The Cancer Research UK/MRC Oxford Institute for Radiation Oncology is supported by core grants from the Medical Research Council and Cancer Research UK.

GSH has been supported by Cancer Research UK Clinician Scientist Awards (grant numbers C34326/A13092 and C34326/A19590).

CONFLICT OF INTEREST

The authors declare no conflict of interest.

REFERENCES

- Abe Y, Matsumoto S, Kito K, Ueda N (2000) Cloning and expression of a novel MAPKK-like protein kinase, lymphokine-activated killer T-cell-originated protein kinase, specifically expressed in the testis and activated lymphoid cells. *J Biol Chem* **275**: 21525–21531.
- Abe Y, Takeuchi T, Kagawa-Miki L, Ueda N, Shigemoto K, Yasukawa M, Kito K (2007) A mitotic kinase TOPK enhances Cdk1/cyclin B1-dependent phosphorylation of PRC1 and promotes cytokinesis. *J Mol Biol* **370**: 231–245.
- Andreassen PR, Lacroix FB, Lohez OD, Margolis RL (2001) Neither p21WAF1 nor 14-3-3sigma prevents G2 progression to mitotic catastrophe in human colon carcinoma cells after DNA damage, but p21WAF1 induces stable G1 arrest in resulting tetraploid cells. *Cancer Res* **61**: 7660–7668.
- Ayllon V, O'Connor R (2007) PBK/TOPK promotes tumour cell proliferation through p38 MAPK activity and regulation of the DNA damage response. *Oncogene* **26**: 3451–3461.
- Brown-Clay JD, Shenoy DN, Timofeeva O, Kallakury BV, Nandi AK, Banerjee PP (2015) PBK/TOPK enhances aggressive phenotype in prostate cancer via beta-catenin-TCF/LEF-mediated matrix metalloproteinases production and invasion. *Oncotarget* **6**: 15594–15609.
- Dearnaley D, Syndikus I, Mossop H, Khoo V, Birtle A, Bloomfield D, Graham J, Kirkbride P, Logue J, Malik Z, Money-Kyrle J, O'Sullivan JM, Panades M, Parker C, Patterson H, Scrase C, Staffurth J, Stockdale A, Tremlett J, Bidmead M, Mayles H, Naismith O, South C, Gao A, Cruickshank C, Hassan S, Pugh J, Griffin C, Hall E, CHHiP Investigators (2016) Conventional versus hypofractionated high-dose intensity-modulated radiotherapy for prostate cancer: 5-year outcomes of the randomised, non-inferiority, phase 3 CHHiP trial. *Lancet Oncol* **17**: 1047–1060.
- Deckbar D, Birraux J, Krempler A, Tchouandong L, Beucher A, Walker S, Stiff T, Jeggo P, Lobrich M (2007) Chromosome breakage after G2 checkpoint release. *J Cell Biol* **176**: 749–755.
- Dillon MT, Good JS, Harrington KJ (2014) Selective targeting of the G2/M cell cycle checkpoint to improve the therapeutic index of radiotherapy. *Clin Oncol (R Coll Radiol)* **26**: 257–265.
- Dou X, Wei J, Sun A, Shao G, Childress C, Yang W, Lin Q (2015) PBK/TOPK mediates geranylgeranylation signaling for breast cancer cell proliferation. *Cancer Cell Int* **15**: 27.
- Fujibuchi T, Abe Y, Takeuchi T, Ueda N, Shigemoto K, Yamamoto H, Kito K (2005) Expression and phosphorylation of TOPK during spermatogenesis. *Dev Growth Differ* **47**: 637–644.
- Garrett MD, Collins I (2011) Anticancer therapy with checkpoint inhibitors: what, where and when? *Trends Pharmacol Sci* **32**: 308–316.
- Gaudet S, Branton D, Lue RA (2000) Characterization of PDZ-binding kinase, a mitotic kinase. *Proc Natl Acad Sci USA* **97**: 5167–5172.
- Hanahan D, Weinberg RA (2011) Hallmarks of cancer: the next generation. *Cell* **144**: 646–674.
- He F, Yan Q, Fan L, Liu Y, Cui J, Wang J, Wang L, Wang Y, Wang Z, Guo Y, Huang G (2010) PBK/TOPK in the differential diagnosis of cholangiocarcinoma from hepatocellular carcinoma and its involvement in prognosis of human cholangiocarcinoma. *Hum Pathol* **41**: 415–424.
- Lei B, Liu S, Qi W, Zhao Y, Li Y, Lin N, Xu X, Zhi C, Mei J, Yan Z, Wan L, Shen H (2013) PBK/TOPK expression in non-small-cell lung cancer: its correlation and prognostic significance with Ki67 and p53 expression. *Histopathology* **63**: 696–703.
- Lei B, Qi W, Zhao Y, Li Y, Liu S, Xu X, Zhi C, Wan L, Shen H (2015) PBK/TOPK expression correlates with mutant p53 and affects patients' prognosis and cell proliferation and viability in lung adenocarcinoma. *Hum Pathol* **46**: 217–224.
- Matsumoto S, Abe Y, Fujibuchi T, Takeuchi T, Kito K, Ueda N, Shigemoto K, Gyo K (2004) Characterization of a MAPKK-like protein kinase TOPK. *Biochem Biophys Res Commun* **325**: 997–1004.
- Matsuo Y, Park JH, Miyamoto T, Yamamoto S, Hisada S, Alachkar H, Nakamura Y (2014) TOPK inhibitor induces complete tumor regression in xenograft models of human cancer through inhibition of cytokinesis. *Sci Transl Med* **6**: 259ra145.
- Nandi AK, Ford T, Fleksher D, Neuman B, Rapoport AP (2007) Attenuation of DNA damage checkpoint by PBK, a novel mitotic kinase, involves protein-protein interaction with tumor suppressor p53. *Biochem Biophys Res Commun* **358**: 181–188.
- Ohashi T, Komatsu S, Ichikawa D, Miyamae M, Okajima W, Imamura T, Kiuchi J, Kosuga T, Konishi H, Shiozaki A, Fujiwara H, Okamoto K, Tsuda H, Otsuji E (2017) Overexpression of PBK/TOPK relates to tumour malignant potential and poor outcome of gastric carcinoma. *Br J Cancer* **116**: 218–226.
- O'Leary PC, Penny SA, Dolan RT, Kelly CM, Madden SF, Rexhepaj E, Brennan DJ, McCann AH, Ponten F, Uhlen M, Zagorodzon R, Duffy MJ, Kell MR, Jirstrom K, Gallagher WM (2013) Systematic antibody generation and validation via tissue microarray technology leading to identification of a novel protein prognostic panel in breast cancer. *BMC Cancer* **13**: 175.
- Orthwein A, Fradet-Turcotte A, Noordermeer SM, Canny MD, Brun CM, Strecker J, Escribano-Diaz C, Durocher D (2014) Mitosis inhibits DNA double-strand break repair to guard against telomere fusions. *Science* **344**: 189–193.
- Park JH, Jeong YJ, Won HK, Choi SY, Park JH, Oh SM (2014) Activation of TOPK by lipopolysaccharide promotes induction of inducible nitric oxide synthase through NF-kappaB activity in leukemia cells. *Cell Signal* **26**: 849–856.
- Park JH, Lin ML, Nishidate T, Nakamura Y, Katagiri T (2006) PDZ-binding kinase/T-LAK cell-originated protein kinase, a putative cancer/testis antigen with an oncogenic activity in breast cancer. *Cancer Res* **66**: 9186–9195.
- Park JH, Nishidate T, Nakamura Y, Katagiri T (2010) Critical roles of T-LAK cell-originated protein kinase in cytokinesis. *Cancer Sci* **101**: 403–411.
- Rhodes DR, Kalyana-Sundaram S, Mahavisno V, Varambally R, Yu J, Briggs BB, Barrette TR, Anstet MJ, Kincaid-Beal C, Kulkarni P, Varambally S, Ghosh D, Chinnaiyan AM (2007) Oncomine 3.0: genes, pathways, and networks in a collection of 18,000 cancer gene expression profiles. *Neoplasia* **9**: 166–180.
- Rizkallah R, Batsomboon P, Dudley GB, Hurt MM (2015) Identification of the oncogenic kinase TOPK/PBK as a master mitotic regulator of C2H2 zinc finger proteins. *Oncotarget* **6**: 1446–1461.
- Shih MC, Chen JY, Wu YC, Jan YH, Yang BM, Lu PJ, Cheng HC, Huang MS, Yang CJ, Hsiao M, Lai JM (2012) TOPK/PBK promotes cell migration via modulation of the PI3K/PTEN/AKT pathway and is associated with poor prognosis in lung cancer. *Oncogene* **31**: 2389–2400.
- Shinde SR, Gangula NR, Kavela S, Pandey V, Maddika S (2013) TOPK and PTEN participate in CHFR mediated mitotic checkpoint. *Cell Signal* **25**: 2511–2517.
- Steigemann P, Wurzenberger C, Schmitz MH, Held M, Guizetti J, Maar S, Gerlich DW (2009) Aurora B-mediated abscission checkpoint protects against tetraploidization. *Cell* **136**: 473–484.
- Sun H, Zhang L, Shi C, Hu P, Yan W, Wang Z, Duan Q, Lu F, Qin L, Lu T, Xiao J, Wang Y, Zhu F, Shao C (2015) TOPK is highly expressed in circulating tumor cells, enabling metastasis of prostate cancer. *Oncotarget* **6**: 12392–12404.
- Terzoudi GI, Manola KN, Pantelias GE, Iliakis G (2005) Checkpoint abrogation in G2 compromises repair of chromosomal breaks in ataxia telangiectasia cells. *Cancer Res* **65**: 11292–11296.
- Tiwana GS, Prevo R, Buffa FM, Yu S, Ebner DV, Howarth A, Folkes LK, Budwal B, Chu KY, Durrant L, Muschel RJ, McKenna WG, Higgins GS (2015) Identification of vitamin B1 metabolism as a tumor-specific radiosensitizing pathway using a high-throughput colony formation screen. *Oncotarget* **6**: 5978–5989.
- Visconti R, Della Monica R, Grieco D (2016) Cell cycle checkpoint in cancer: a therapeutically targetable double-edged sword. *J Exp Clin Cancer Res* **35**: 153.
- Xiao YC, Yang ZB, Cheng XS, Fang XB, Shen T, Xia CF, Liu P, Qian HH, Sun B, Yin ZF, Li YF (2015) CXCL8, overexpressed in colorectal cancer, enhances the resistance of colorectal cancer cells to anoikis. *Cancer Lett* **361**: 22–32.

Zlobec I, Molinari F, Kovac M, Bihl MP, Altermatt HJ, Diebold J, Frick H, Germer M, Horcic M, Montani M, Singer G, Yurtsever H, Zettl A, Terracciano L, Mazzucchelli L, Saletti P, Frattini M, Heinimann K, Lugli A (2010) Prognostic and predictive value of TOPK stratified by KRAS and BRAF gene alterations in sporadic, hereditary and metastatic colorectal cancer patients. *Br J Cancer* **102**: 151–161.

Zykova TA, Zhu F, Lu C, Higgins L, Tatsumi Y, Abe Y, Bode AM, Dong Z (2006) Lymphokine-activated killer T-cell-originated protein kinase phosphorylation of histone H2AX prevents arsenite-induced apoptosis in RPMI7951 melanoma cells. *Clin Cancer Res* **12**: 6884–6893.

Zykova TA, Zhu F, Vakorina TI, Zhang J, Higgins LA, Urusova DV, Bode AM, Dong Z (2010) T-LAK cell-originated protein kinase (TOPK) phosphorylation of Prx1 at Ser-32 prevents UVB-induced apoptosis in RPMI7951 melanoma cells through the regulation of Prx1 peroxidase activity. *J Biol Chem* **285**: 29138–29146.



This work is licensed under the Creative Commons Attribution 4.0 International License. To view a copy of this license, visit <http://creativecommons.org/licenses/by/4.0/>

© The Author(s) named above 2017

Supplementary Information accompanies this paper on British Journal of Cancer website (<http://www.nature.com/bjc>)